

Mini-Report #7

**A ONE-DIMENSIONAL NUMERICAL MODEL FOR ANALYSIS OF
STEADY-STATE VARIABLE DENSITY GROUND WATER FLOW**

Basalt Waste Isolation Project
Subtask 2.5
Numerical Evaluation of Conceptual Models

Prepared by

Terra Therma Inc.

for

Nuclear Waste Consultants

December, 1986



TERRA THERMA, INC.

WATER CONSULTANTS AND ENGINEERS

8702200344 870108
PDR WMRES EECNWC I
D-1021 PDR

TABLE OF CONTENTS

	Page
1.0 INTRODUCTION	1
1.1 RELEVANCE TO NRC	3
1.2 RELATIONSHIP TO OTHER SITE CHARACTERIZATION/REGULATORY TASKS ...	5
2.0 OBJECTIVE	7
3.0 EVALUATION	7
3.1 OPERATIONAL APPROACH	7
3.2 CONCEPTUAL MODEL FOR BWIP	8
3.2.1 Framework	8
3.2.2 Flow System	9
3.3 TECHNICAL APPROACH	9
3.3.1 Solution Techniques	9
3.3.2 Assumptions	11
4.0 ANALYSIS	12
4.1 BASIC RELATIONSHIPS	12
4.1.1 True (Theoretical) Hydraulic Head	12
4.1.2 Other Techniques For Expressing Hydraulic Head	13
4.1.3 Functional Relationship Between Density and Temperature .	15
4.1.4 Functional Relationship Between Viscosity and Temperature	17
4.2 NUMERICAL SIMULATION	18
4.2.1 Finite Difference Discretization	19
4.2.2 Solution Technique	21
4.2.3 Calculation of Heads	22
4.3 EXAMPLE SIMULATION FOR BWIP	24
4.4 RESULTS	25
5.0 CONCLUSIONS	27
6.0 DISCUSSION	28
7.0 REFERENCES	29

LIST OF TABLES

	Page
TABLE 1. NOMENCLATURE	30
TABLE 2. DENSITY OF PURE WATER AT DIFFERENT TEMPERATURES AND PRESSURES ..	32
TABLE 3. VISCOSITY OF PURE WATER AT DIFFERENT TEMPERATURES AND PRESSURES	33
TABLE 4. EXAMPLE SIMULATION PERFORMED IN THIS STUDY	34
TABLE 5. PRINTOUT FROM EXAMPLE SIMULATION	35

LIST OF FIGURES

	Page
FIGURE 1. TEMPERATURE VS. DENSITY OF PURE WATER AT DIFFERENT PRESSURES ..	37
FIGURE 2. PRESSURE CORRECTION FOR DENSITY OF PURE WATER	38
FIGURE 3. TEMPERATURE VS. VISCOSITY OF PURE WATER	39
FIGURE 4. FINITE DIFFERENCE DISCRETIZATION	40
FIGURE 5. ITERATIVE SOLUTION FLOW CHART	41
FIGURE 6. FINITE DIFFERENCE MODEL USED IN EXAMPLE SIMULATION	42
FIGURE 7. HEAD PLOTS FROM EXAMPLE SIMULATION	43

1.0 INTRODUCTION

Hydrologic characterization at the BWIP site involves activities directed towards developing an understanding of the ground water flow system in Columbia River Basalt. It has long been recognized in the hydrologic and petroleum literature that variable density fluids in ground water systems can have a significant impact on flow directions and flux rates. For pre-emplacement conditions, fluid density can be affected by the natural distribution of temperature (geothermal gradient) and salinity. The effects of variable density ground water on interpreting flow for pre-emplacement (current) conditions will have to be evaluated. For post-emplacement conditions, the heat generated by high level waste will result in major thermal perturbations that may persist long after the rate of heat generation has been reduced to minimum levels. The temperature changes associated with this process, including temperature effects on fluid density, will have significant impacts on the hydrodynamics of ground water flow in the vicinity of a waste repository. Temperature induced variable density flow needs to be considered in post-emplacement performance modeling of the BWIP site.

Recognizing the importance of temperature induced, variable density flow on repository performance modeling, DOE and NRC have developed several ground water flow numerical models which can incorporate temperature effects (e.g., PORFLO, SWIFT). Unfortunately, setting up these models tends to be very time consuming and they are expensive to operate, requiring the use of mainframe

computers. While such complicated codes may be ultimately be required for site performance modeling, they tend to be of little practical use for sensitivity analyses which can require numerous simulations. For this purpose, less complicated and more efficient algorithms can have definite advantages, provided that they give realistic and/or conservative results.

This mini-report develops a methodology for analyzing one-dimensional (vertical), variable density ground water flow in a porous medium. The technique is based on a steady-state finite difference numerical model which is programmed on the spreadsheet program LOTUS 123. The program is designed to run efficiently on an IBM PC microcomputer and can take advantage of graphic capabilities built into LOTUS. The numerical algorithm is based on an iterative (trial and error) procedure that converges to a unique solution.

The model developed in this study differs from the above mentioned mainframe codes in that it does not consider coupled ground water - heat flow (i.e., convection). However, analyses by Codell (1983) indicate that convection can be safely neglected in a basalt repository. Thus, heat transport is dominated by simple conduction which is completely decoupled from ground water flow and can be calculated independently. To incorporate the effects of heat into this model, temperature distributions are first specified apriori as input to the model. The code then calculates fluid density and viscosity at each point using empirical equations with temperature as the independent variable.

1.1 RELEVANCE TO NRC

As described in Section 10 CFR 60.122 (a) (1), qualitative siting criteria have been developed by the NRC which require the license application to provide information that can be used to assess "reasonable assurance" that performance objectives will be met. These siting criteria are based on pre-
emplacement/post-emplacement conditions and are categorized in terms of "favorable" and "potentially adverse" conditions. The conditions relevant to BWIP which require a knowledge of pre-emplacement ground water flow are listed below:

Favorable Conditions

122(b)(7) "Pre-emplacement groundwater travel time [GWTT] ... that substantially exceeds 1,000 years."

Potentially Adverse Conditions

122(c)(2) "Potential for foreseeable human activity to adversely affect the groundwater flow system, such as ground water withdrawals, extensive irrigation, subsurface injection of fluids, [repository heat] ..."

122(c)(5) "Potential for changes in hydrologic conditions that would affect the migration of radionuclides ..."

With regard to ground water flow, "favorable conditions" are based on pre-emplacment conditions within the hydrogeologic system. "Potentially adverse conditions" generally require an evaluation of changes in ground water flow resulting from natural and man-made phenomena. Since both pre- and post-emplacment conditions at BWIP involve the presence of variable density ground water, the effects of variable density need to be considered in evaluating the siting criteria.

In addition to the above qualitative siting criteria, the NRC has formulated performance objectives in Section 10 CFR 60.111-60.113. With regard to ground water flow, the EPA Cumulative Flux Standard specifies the amount of radionuclides which can reach the accessible environment over a period of 10,000 years. Since temperature changes may be significant during this post-emplacment period, the effects of repository heat on radionuclide transport will have to be addressed. As a consequence, performance models will need to incorporate the effects of variable temperature on ground water density and viscosity.

1.2 RELATIONSHIP TO OTHER SITE CHARACTERIZATION/REGULATORY TASKS

An important factor in assessing the suitability of the BWIP site is application of the GWTT criterion. To date, both DOE and NRC have placed a high degree of importance on this regulatory standard for evaluating high level waste sites. GWTT requires an estimate of the velocity of ground water flow along the "fastest" path between the repository and accessible environment. Since variable density ground water currently exists within the hydrogeologic system, its effects on flow path and velocity will have to be evaluated.

Another factor in assessing the suitability of the BWIP site is application of the EPA Cumulative Flux Standard. This regulatory criterion will require an understanding and quantification of the flow field under post-emplacement conditions. Since thermal effects may cause significant variations in hydraulic gradients, buoyancy forces, and fluid viscosity, the impact of repository heat on ground water flow will be an important consideration in applying this regulatory standard.

DOE is currently formulating its plans for future testing and analysis at the BWIP site. These activities will probably result in extension of the Baseline Monitoring Program, evaluation of data obtained from the monitoring installations, and application of this data (interpreted heads) to GWTT and other regulatory criteria. Evaluation of the effects of fluid density on

hydraulic heads at the BWIP site can therefore provide important insights in developing and implementing future site characterization activities.

2.0 OBJECTIVE

The objective of this study is to develop an efficient, one-dimensional (vertical) numerical model which can incorporate the effects of variable fluid density and viscosity on ground water flow. The model should use input values of temperature to determine fluid density and viscosity at any point within the flow system.

3.0 EVALUATION

3.1 OPERATIONAL APPROACH

The numerical model developed herein analyzes ground water flow in a variable density system with simple geometry. Empirical equations used by the model to relate temperature to fluid density and viscosity are consistent with known characteristics at the BWIP site. The purposed use of this model is not to simulate ground water flow at BWIP in detail, but rather to assess (in a sensitivity manner) the importance of temperature (and fluid density) on ground water flow characteristics.

The model calculates various types of hydraulic "heads" used by hydrologists to characterize ground water flow. These include:

- Fresh water head

- Environmental head
- Observation well or piezometer water level
- Hydraulic head based on the theoretical definition (true head)

Thus, the model can be used to assess the reliability of the above techniques for characterizing ground water flow in the variable density flow system at BWIP.

3.2 CONCEPTUAL MODEL FOR BWIP

3.2.1 Framework

The candidate repository horizon is situated within Columbia River Basalt at a depth of about 960 meters below ground surface. For proposed simulations, only vertical flow is considered. Thus, the physical system is composed of an alternating sequence of relatively high permeability interflows separated by low permeability flow interiors, with the ground water flow direction perpendicular to bedding. Analytically, this heterogeneous system is replaced by a homogeneous medium having an equivalent vertical permeability. Explicit incorporation of basalt heterogeneities is possible with the numerical approach developed in this study. Simulating a more complex (heterogeneous) system of this type will be considered in a future mini-report.

3.2.2 Flow System

Ground water flow within the geologic medium is treated as steady state and one dimensional (vertical). Flow is driven by the vertical pressure distribution and buoyancy forces (resulting variations in fluid density). The density of ground water is dependent on temperature and salinity, both of which can have any arbitrary vertical distribution with depth.

The assumption of one-dimensional vertical flow may be a major limitation in the analysis presented herein. It is generally felt that ground water flow at the BWIP site has strong horizontal components, particularly within the high permeability interflows. Extension of the analytical approach developed in this study to two dimensional planar and axisymmetric flow systems will be considered in future mini-reports.

3.3 TECHNICAL APPROACH

3.3.1 Solution Techniques

Darcy's law for a variable density fluid provides the basis for this numerical model. The vertical component of flow can be expressed as follows (Runchal et al, 1985):

$$q_z = - \frac{k D}{u} \frac{g}{\rho} \left(\frac{dH}{dz} + R \right) \quad (1)$$

where:

$$H = \frac{p}{D_o g} + E \quad (2)$$

$$R = \frac{D}{D_o} - 1 \quad (3)$$

qz = vertical specific discharge (Darcy velocity) $[L \ t^{-1}]$

k = intrinsic permeability $[L^2]$

D = fluid density $[M \ L^{-3}]$

g = acceleration of gravity $[L \ t^{-2}]$

u = fluid viscosity $[M \ L^{-1} \ t^{-1}]$

z = vertical coordinate $[L]$

p = fluid pressure $[M \ L^{-1} \ t^{-2}]$

E = elevation above arbitrary datum $[L]$

D_o = arbitrary reference density $[M \ L^{-3}]$

Because the reference density is commonly taken as 1 g cm^{-3} , the parameter H is sometimes referred to as a fresh water head. By definition, this parameter is directly related to fluid pressure.

For a variable density system, it is required that mass be conserved rather than flow volume. This is because the mass of water associated with a given fluid volume will change as a function of density. Mass flux rate is expressed as:

$$M_z = qz D \quad (4)$$

where:

M_z = vertical mass flux rate per unit area $[M \ t^{-1} \ L^{-2}]$

Substituting (4) into (1) gives Darcy's law expressed in terms of mass flux:

$$Mz = - \frac{k D^2 g}{u} \left(\frac{dH}{dz} + R \right) \quad (5)$$

3.3.2 Assumptions

Principal assumptions associated with the numerical model developed in this study are as follows:

1. Ground water flow is one dimensional (vertical) and steady state. Horizontal flow components are not considered.
2. Fractured rock is treated mathematically as an equivalent porous medium (continuum).
3. Temperature and salinity distributions are not affected by ground water flow (i.e., convection is not considered).
4. The flow system does not contain internal sources or sinks.

4.0 ANALYSIS

4.1 BASIC RELATIONSHIPS

4.1.1 True (Theoretical) Hydraulic Head

Quantitative evaluation of water level/pressure data requires that these measurements can be converted to hydraulic parameters describing the hydrodynamics of ground water flow. Traditionally, ground water hydrology studies have used the concept of "hydraulic head" as a scalar quantity representing the energy potential for flow at any given point in the system.

Hydraulic head is defined from potential theory by the following equation (Hubbert, 1940):

$$h_t(x,y,z) = h_o + (z-z_o) + \frac{1}{g} \int_{p_o}^{p(x,y,z)} \frac{1}{D(p)} dp \quad (6)$$

where:

h_t = theoretical or true hydraulic head [L]
 p = fluid pressure [M L⁻¹ t⁻²]
 D = fluid density [M L⁻³]
 z = vertical coordinate [L]
 g = acceleration of gravity [L t⁻²]

In the above equation, $D(p)$ represents a functional relationship between density and pressure, including the effects of temperature and salinity. Also,

p_o and z_o are the fluid pressure and vertical coordinate, respectively, for an arbitrary "reference state" at which hydraulic head is assigned a value equal to h_o (reference head).

4.1.2 Other Techniques for Expressing Hydraulic Head

In variable density systems, it is generally difficult to apply the theoretical definition of true hydraulic head due to an uncertain knowledge of functional relationship between density and pressure. As a result, alternative techniques have been proposed. These techniques are discussed below.

FRESH WATER HEAD

Fresh water head is defined by the following equation:

$$h_f(x,y,z) = h_o + (z - z_o) + \frac{p(x,y,z) - p_o}{\rho_o g} \quad (7)$$

where:

h_f = fresh water head [L]
 ρ_o = reference fluid density [M L⁻³]

and other parameters are defined previously (refer to list of nomenclature in Table 1). The above equation follows from the definition of true head (Equation 6) for the case where density is a constant equal to the reference density. The term fresh water head is used because the reference density is usually taken to be 1 g cm⁻³. However, the reference density can be any arbitrary value.

Generally, the reference head, reference coordinate, and reference pressure (h_0 , z_0 , and p_0 , respectively) are set equal to zero and z is defined as the elevation relative to mean sea level (MSL). In this case, Equation 7 becomes:

$$h_f(x,y,z) = E + \frac{p(x,y,z)}{\rho_0 g} \quad (8)$$

where:

E = elevation relative to MSL [L]

ENVIRONMENTAL HEAD

Environmental head is defined as follows:

$$h_e(x,y,z) = h_0 + (z - z_0) + \frac{p(x,y,z) - p_0}{\rho(x,y,z) g} \quad (9)$$

where:

h_e = environmental head [L]

and constant density (ρ) is set equal to the actual fluid density existing at the point of pressure measurement. Setting h_0 , z_0 , and p_0 equal to zero and defining z in terms of elevation, Equation (9) becomes:

$$h_e(x,y,z) = E + \frac{p(x,y,z)}{\rho(x,y,z) g} \quad (10)$$

PIEZOMETER WATER LEVEL

In many hydrologic studies, it is assumed that the equilibrium water level in a piezometer or observation well represents a reliable measure of the hydraulic

head existing at the completion interval. Water level (hw) in a piezometer is contained in the following relationship:

$$p(x,y,z) = g \int_z^{hw} D_w(z) dz \quad (11)$$

where:

hw = water level in piezometer with completion interval at
(x,y,z) [L]

Dw = fluid density inside the borehole [M L⁻³]

If z is defined in terms of elevation, the water level will also be expressed as an elevation. The term D(z) represents the functional relationship between fluid density inside the borehole and elevation.

4.1.3 Functional Relationship Between Density and Temperature

For this mini-report (and others to follow), it is desirable to develop an empirical relationship between density, temperature, and pressure which covers the range of pre- and post-emplacement conditions expected at BWIP. A general equation for density is given by:

$$D = A(T) + B(P) \quad (12)$$

where:

D = density of pure water [g cm⁻³]

T = temperature [C]

P = pressure [bar]

and A and B represent empirical functions. In the above equation, A(T) provides values of density (as a function of temperature) at a standard pressure of one bar, and B(P) is a correction factor to account for pressures greater than one bar. The polynomial function for by A(T) is (Weast, 1986):

$$A(T) = \left(+999.83952 + 16.945176 T - 7.9870401 \times 10^{-3} T^2 - 46.170461 \times 10^{-6} T^3 + 105.56302 \times 10^{-9} T^4 - 280.54253 \times 10^{-12} T^5 \right) / \left(1 + 16.879850 \times 10^{-3} T \right) / 1000 \quad (13)$$

In Table 2, densities predicted by A(T) are compared with true values of density at different temperatures and pressures. These data are plotted in Figure 1. For a standard pressure of one bar, A(T) is accurate to about four significant figures. It is observed in Table 2 that the difference between A(T) and true density is more or less uniform for a given pressure. Thus, the correction factor B(P) is obtained by calculating the average difference between A(T) and true density for different temperatures at a prescribed pressure. Values of the correction factor are shown at the bottom of Table 2 and are plotted in Figure 2. Linear regression on this data results in the following empirical relationship for the pressure correction:

$$B(P) = 4.628 \times 10^{-5} P + .000018 \quad (14)$$

Using the above relationships for A(T) and B(T), densities accurate to three significant figures can be calculated for a temperature range of 0 to 150 degrees Celsius and a pressure range of 1 to 100 bars.

For the numerical model developed in this study, it is preferable to use a density equation based solely on temperature. A single-valued correction factor can be defined as the value of B given at a pressure of 50 bars:

$$B^* = B(50 \text{ bar}) = 0.00233 \text{ g cm}^{-3} \quad (15)$$

where:

$$B^* = \text{general pressure correction for water density} \\ (0.00233 \text{ g cm}^{-3})$$

Thus, in this mini-report, density is calculated by the following general equation:

$$D = A(T) + B^* \quad (16)$$

Values from the general equation are given in Table 1 and compared graphically to true density values in Figure 1. Errors introduced by assuming a constant-valued pressure correction are not expected to be significant for the anticipated uses of the numerical model.

4.1.4 Functional Relationship Between Viscosity and Temperature

Water viscosity is strongly dependent on temperature, but not particularly sensitive to pressure. An empirical equation relating viscosity of pure water to temperature is given by (adapted from Weast, 1986):

$$u = C(T) \quad (17)$$

$$C(T) = \frac{u_{20}}{2.30259} \exp \left[\frac{1.3272 (20-T) - 0.001053 (T-20)^2}{T + 105} \right] \quad (18)$$

where:

u = water viscosity [poise = $\text{g cm}^{-1} \text{ s}^{-1}$]
 u_{20} = water viscosity at 20 degrees C (0.01002 poise)
 T = temperature [C]

In Table 3, predicted water viscosity from the above equation is compared to true viscosity values at pressures of 1 and 100 bars. Graphical comparison of this data is provided in Figure 3. At one bar, Equation 17 is accurate to about three significant figures. The one viscosity value obtained for a pressure of 100 bars, suggests that water viscosity is insensitive to pressure. Therefore, a pressure correction is considered unnecessary for the purpose of this study. For the numerical model developed herein, Equation 17 is used to predict water viscosity for a given temperature.

4.2 NUMERICAL SIMULATION

For steady-state flow, the following equation must be solved, subject to appropriate boundary conditions:

$$\text{DEL } M = 0 \quad (19)$$

where:

M = mass flux rate per unit area [$\text{M t}^{-1} \text{ L}^{-2}$]

This equation is a statement of conservation of mass for fluid within the flow region. For one dimensional vertical flow, Equation (19) reduces to:

$$M_z = \text{constant} \quad (20)$$

where M_z is given by Darcy's law expressed in Equations (2), (3), and (5). Due to the nonlinear nature of Equation (5), resulting from variations in density and viscosity, simulation of ground water flow requires numerical techniques.

4.2.1 Finite Difference Discretization

Numerical simulation is accomplished by discretizing the system into N finite difference elements ($n = 1, 2, 3 \dots N$) as shown in Figure 4. Boundary conditions at the top and bottom of the mesh are those of prescribed fresh water head (defined in Equation 2). Material and fluid properties are assumed to be uniform within each element and a constant value of intrinsic permeability is assigned throughout the flow system. Values of density and viscosity in each element are based on input values of temperature/salinity, and make use of Equations (16) and (17):

$$D(n) = A[T(n)] + B^* + S(n) \quad (21)$$

$$\mu(n) = C[T(n)] \quad (22)$$

where:

- n = element number []
- $D(n)$ = average fluid density in element n [$M L^{-3}$]
- $\mu(n)$ = average fluid viscosity in element n [$M L^{-1} t^{-1}$]
- $T(n)$ = average temperature in element n [T]
- $S(n)$ = average ground water salinity (TDS) in element n [$g\ cm^{-3}$]

A total of $N+1$ nodes ($j = 0, 1, 2 \dots N$) exist at the boundary between each element and at the top and bottom of the mesh (refer to Figure 4). At the boundary nodes:

$$H(0) = H' \quad (23)$$

$$H(N) = H'' \quad (24)$$

where:

H' = prescribed fresh water head at the top of the flow system [L]
 $H(0)$ = fresh water head assigned to node 0 [L]
 H'' = prescribed fresh water head at the bottom of the flow system [L]
 $H(N)$ = fresh water head assigned to node N [L]

Within each element, the mass flux rate is given by:

$$M(n) = - \frac{k g D(n)^2}{u(n)} \left[\frac{H(j-1) - H(j)}{b} + R(n) \right] \quad n = 1, 2, 3 \dots N \text{ and } j = n \dots (25)$$

$$H(j) = \frac{p(j)}{D_o g} + E(j) \quad (26)$$

$$R(n) = \frac{D(n)}{D_o} - 1 \quad (27)$$

where:

n = element number
 j = node number
 $M(n)$ = mass flux in element n [$M t^{-1} L^{-2}$]
 k = intrinsic permeability (constant for all elements) [L^2]
 g = acceleration of gravity [$L t^{-2}$]
 $H(j)$ = reference head at node j [L]
 D_o = reference density [$M L^{-3}$]
 b = distance between nodes [L]
 $p(j)$ = pressure at node j [$M L^{-1} t^{-2}$]
 $E(j)$ = elevation at node j [L]

Equations (25), (26), and (27) represent the finite difference approximations to (5), (2), and (3), respectively.

For steady state the correct distribution of fresh water heads are obtained (i.e., solution achieved) when the calculated mass flux is constant within each element:

$$M(n) = \text{constant} \quad n = 1, 2, 3 \dots N \quad (28)$$

4.2.2 Solution Technique

An iterative solution procedure is used to adjust fresh water heads until Equation (28) is satisfied (flux rate constant in each element). A flow chart describing the solution technique is shown in Figure 5. The predicted head at each node is determined by:

$$H(0)^{i+1} = H' \quad (29)$$

$$H(j)^{i+1} = H' + \sum_{n=1}^j b \left[- \frac{M^*(n) u(n)}{k g D(n)^2} - R(n) \right] \quad j = 1, 2, 3 \dots N-1 \quad (30)$$

$$H(N)^{i+1} = H'' \quad (31)$$

where:

$$M^*(n) = (1-w) M(n)^i + w M_{av}^i \quad (32)$$

i = iteration number []

$M^*(n)$ = predicted mass flux rate in element n [$M \text{ t}^{-1} \text{ L}^{-2}$]

$M(n)^i$ = calculated mass flux rate in element n for iteration i [$M \text{ t}^{-1} \text{ L}^{-2}$]

M_{av}^i = average value of mass flux rate over all elements for iteration i [$M \text{ t}^{-1} \text{ L}^{-2}$]

w = weighting factor to improve convergence ($0 < w < 1$) []

and SUM represents a summation. The iterative process is continued until $M(n)^i$ approaches the same value for each element.

4.2.3 Calculation of Heads

FRESH WATER HEAD

Fresh water heads at each node are directly computed by the finite difference equations:

$$hf(j) = H(j) \quad (33)$$

where:

$$hf(j) = \text{fresh water head at node } j \text{ [L]}$$

ENVIRONMENTAL HEAD

Environmental heads are computed as follows:

$$he(j) = \frac{p(j)}{D(j)g} + E(j) \quad (34)$$

$$p(j) = [H(j) - E(j)] D_o g \quad (35)$$

where:

$$\begin{aligned} he(j) &= \text{environmental head at node } j \text{ [L]} \\ p(j) &= \text{pressure at node } j \text{ [M L}^{-1} \text{ t}^{-2}] \\ D(j) &= \text{fluid density at node } j \text{ [M L}^{-3}] \end{aligned}$$

TRUE HEAD

To calculate the true (theoretical) hydraulic head, the integral in Equation (6) is evaluated in a discretized manner:

$$ht(j) = h_0 + (z - z_0) + \frac{1}{g} \sum_{m=1}^j \frac{p(m) - p(m-1)}{D(n)} \quad (36)$$

where:

m = node number

ht(j) = true hydraulic head at node j [L]

For calculating true hydraulic head, the reference state is positioned at the top of the flow system where the reference head is arbitrarily set equal to the environmental head. Thus,

$$ht(j) = h_e(0) + (E(j) - E(0)) + \frac{1}{g} \sum_{m=1}^j \frac{p(m) - p(m-1)}{D(n)} \quad (37)$$

PIEZOMETER WATER LEVEL

In calculating piezometer water level, salinity at any location inside the borehole is assumed equal to the formation salinity at the zone of completion. This situation is likely to occur if the piezometer was developed by pumping and/or if ionic diffusion has resulted in equalizing salinity within the fluid column to the formation salinity. Thus,

$$Dw(n) = AIT(n) + B^* + S(j) \quad (38)$$

where:

n = element representing segment of borehole

j = node at point of pressure determination (i.e., zone of completion)

Dw(n) = average fluid density inside the borehole within element n [M L⁻³]

Discretizing Equation (11):

$$p(j) = g \sum_{n=2}^j [Dw(n) b] + g [hw(j) - E(1)] Dw(1) \quad (39)$$

where:

$hw(j)$ = water level for piezometer completed at node j [L]

In the above equation, the height of the fluid column (hw) is treated as an unknown in the first (upper-most) element. Solving for hw leads to:

$$hw(j) = E(1) + \frac{p(j) - g b \sum_{n=2}^j Dw(n)}{g Dw(1)} \quad (40)$$

The above equation assumes that the fluid column within and above the first element has a borehole fluid density equal to that existing within the first element [$Dw(1)$].

4.3 EXAMPLE SIMULATION FOR BWIP

The finite difference formulation described above was programed on LOTUS 123 and operated on an IBM compatible personal computer. The general approach for using spreadsheet programs to construct ground water models is described by Olsthoorn (1985). The flow region was discretized into twenty-six elements as illustrated in Figure 6. Parameters were chosen to be consistent with known hydrogeologic conditions existing at BWIP.

The top and bottom of the flow system were placed at the Priest Rapids Interflow and Grande Ronde 5 Interflow, respectively. These units have relatively high transmissivity at the RRL and thus, are not likely to experience large changes in pressure as a result of thermally induced flow. Pressure in these units are assumed to remain constant, consistent with the prescribed fresh water head boundary conditions required by the numerical model at the top and bottom of the mesh.

Information pertaining to the example simulation performed in this study is summarized in Table 4. Temperature and salinity were input to have linear distributions with depth. This assumption is valid with regard to temperature, based on the results of borehole logs and the interpreted geothermal gradient. For salinity, the validity of assuming a linear distribution is less certain, but considered appropriate for sensitivity analysis. For this simulation, prescribed fresh water head at the base of the mesh (boundary condition H") was adjusted until piezometer water level associated with the bottom of the flow system (Grande Ronde 5) was approximately 1.0 meters higher than that existing at the top of the flow system (Priest Rapids). This is consistent with BWIP monitoring data obtained from some of the multiple piezometer installations.

4.4 RESULTS

A printout of model results for the example simulation is given in Table 4 and plots of the various heads vs. elevation are shown in Figure 7. The vertical mass flux predicted by the model is 4.3×10^{-12} g/s/cm² in the positive

(upward) direction. For a fluid density of 1.0 g/cm^3 , this flux rate would correspond to a specific discharge (Darcy velocity) equal to $1.4 \times 10^{-6} \text{ m/yr}$.

5.0 CONCLUSIONS

The steady-state finite difference model developed in this mini-report provides an efficient means for performing simple ground water flow simulations which account for temperature/salinity effects on fluid density. Although the one-dimensional nature of this model does not allow for detailed repository performance modeling, its simplicity and efficiency make it very adaptable for sensitivity analyses. The model calculates mass flux rate through the flow system and provides values of the various types of head at each nodal point. By designing the model on LOTUS 123, input data are easily entered and output can be viewed graphically.

6.0 DISCUSSION

It is anticipated that several future mini-reports will utilize the numerical model described herein. One mini-report will assess the reliability of the various types of head for characterizing pre-emplacement vertical ground water flow directions and flux rates. This analysis will consider effects of the geothermal gradient and vertical salinity distribution on ground water flow. A second mini-report will evaluate the impact of repository heat on vertical ground water flux rates. In that study, vertical temperature distributions will be determined using the one-dimensional variable heat (analytical) solution discussed in Mini-Report #3.

A major limitation of the numerical model is its one dimensional nature. A one dimensional (vertical) approach cannot account for lateral components of flow, which are expected to be significant within basalt interflows. Simulation of this type of flow system will require two dimensional simulations. Extension of the current method to two dimensional planar and axisymmetric problems (with heterogeneity) will be the subject of a future mini-report.

7.0 REFERENCES

- Clark, S.P. (editor) 1966. Handbook of Physical Constants. Geol. Soc. of Amer., Memoir 97.
- Codell, R. 1983. The relative importance of heat transfer by flowing water in high-level waste repositories - I. saturated flow. NRC internal report.
- Hubbert, M.K. 1940. The theory of ground-water motion. Jour. of Geology, vol. 48, no. 8, part 1, pp. 785-944.
- Olsthoorn, T.N. 1985. The power of the electronic spreadsheet: modeling without special programs. Ground Water, vol. 23, no. 3, pp. 381-390.
- Runchal, A.K., B. Sagar, R.G. Baca and N.W. Kline. 1985. PORFLO - a continuum model for fluid flow, heat transfer, and mass transport in porous media. Rockwell Hanford Operations, RHO-BW-CR-150P.
- Weast, R.C. (ed.) 1986. CRC Handbook of Chemistry and Physics. CRC Press, Inc.

TABLE 1. NOMENCLATURE

A(T)	= empirical relationship used to compute water density
b	= distance between nodes [L]
B(p)	= empirical relationship used to correct water density for pressure
C(T)	= empirical relationship used to compute water viscosity
D	= fluid density [M L ⁻³]
D ₀	= arbitrary reference density [M L ⁻³]
D(j)	= fluid density at node j [M L ⁻³]
D(n)	= average fluid density in element n [M L ⁻³]
D(p)	= functional relationship between density and pressure
D _w	= fluid density inside the borehole [M L ⁻³]
D _w (n)	= average fluid density inside the borehole in element n [M L ⁻³]
D _w (z)	= functional relationship between fluid density inside the borehole and elevation
E	= elevation above arbitrary datum (e.g., mean sea level) [L]
E(j)	= height above arbitrary datum at node j [L]
g	= acceleration of gravity [L t ⁻²]
h _e	= environmental head [L]
h _f	= fresh water head [L]
h _t	= theoretical or true hydraulic head [L]
h _w	= water level in piezometer with completion interval at (x,y,z) [L]
h _e (j)	= environmental head at node j [L]
h _f (j)	= reference head at node j [L]
h _t (j)	= true hydraulic head at node j [L]
h _w (j)	= water level for piezometer completed at node j [L]
H'	= prescribed fresh water head at the top of the flow system (boundary condition) [L]
H''	= prescribed fresh water head at the bottom of the flow system (boundary condition) [L]
H(j)	= fresh water head at node j [L]
i	= iteration number []
j	= node number (0,1,2 ... N)
k	= intrinsic permeability [L ²]
m	= node number (0,1,2 ... N)
M	= mass flux rate per unit area [M t ⁻¹ L ⁻²]
M(n)	= mass flux in element n [M t ⁻¹ L ⁻²]
M*(n)	= predicted mass flux rate in element n [M t ⁻¹ L ⁻²]
M(n) ⁱ	= calculated mass flux rate in element n for iteration i [M t ⁻¹ L ⁻²]
M _{av} ⁱ	= average value of mass flux rate over all elements for iteration i [M t ⁻¹ L ⁻²]
n	= element number (1,2,3 ... N)
N	= total number of elements in finite difference mesh
p	= fluid pressure [M L ⁻¹ t ⁻²]
p(j)	= pressure at node j [M L ⁻¹ t ⁻²]
p(m)	= pressure at node m [M L ⁻¹ t ⁻²]
q _z	= vertical specific discharge (Darcy velocity) [L t ⁻¹]

TABLE 1. (cont.)

$S(n)$ = average ground water salinity (TDS) in element n $[M L^{-3}]$
 $S(j)$ = ground water salinity at node j $[M L^{-3}]$
 $T(n)$ = average temperature in element n $[T]$
 μ = fluid viscosity $[M L^{-1} t^{-1}]$
 $\mu(n)$ = average fluid viscosity in element n $[M L^{-1} t^{-1}]$
 w = weighting factor to improve convergence $(0 < w < 1)$ $[-]$
 z = vertical coordinate $[L]$

Note: j and m designate node numbers
 n designates element numbers

TABLE 2. DENSITY OF PURE WATER AT DIFFERENT TEMPERATURES AND PRESSURES

TEMPERATURE VS. DENSITY OF PURE WATER AT DIFFERENT PRESSURES

TEMP. (C)	DENSITY (g/cm ³)								
	EMPIRICAL EQUATION				TRUE VALUES				GENERAL EQUATION
	A(T)	1 BAR	10 BAR	CORREC- TION	50 BAR	CORREC- TION	100 BAR	CORREC- TION	
0	0.9998	0.9999	1.0004	0.0006	1.0025	0.0027	1.0049	0.0051	1.0022
10	0.9997	0.9997	1.0002	0.0005	1.0020	0.0023	1.0042	0.0045	1.0020
20	0.9982	0.9982	0.9987	0.0005	1.0004	0.0022	1.0026	0.0044	1.0005
30	0.9956	0.9957	0.9961	0.0005	0.9979	0.0023	1.0000	0.0044	0.9980
40	0.9922	0.9923	0.9927	0.0005	0.9944	0.0022	0.9965	0.0043	0.9945
50	0.9880	0.9881	0.9885	0.0005	0.9902	0.0022	0.9924	0.0044	0.9904
60	0.9832	0.9832	0.9837	0.0005	0.9854	0.0022	0.9876	0.0044	0.9855
70	0.9776	0.9778	0.9782	0.0004	0.9800	0.0022	0.9822	0.0044	0.9801
80	0.9718	0.9718	0.9723	0.0005	0.9741	0.0023	0.9763	0.0045	0.9741
90	0.9653	0.9653	0.9658	0.0005			0.9699	0.0046	0.9676
100	0.9583	0.9584	0.9589	0.0006	0.9608	0.0025	0.9630	0.0047	0.9606
110	0.9508	***							0.9532
120	0.9429	***	0.9436	0.0007	0.9454	0.0025	0.9479	0.0050	0.9453
130	0.9346	***							0.9369
140	0.9257	***	0.9264	0.0007	0.9286	0.0029	0.9312	0.0055	0.9280
150	0.9164	***							0.9187
PRESSURE (BAR):									
		1	10	50	100				
AV. CORRECTION B(P):		0	0.000533	0.002367	0.004625				

NOTES

EMPIRICAL EQUATION: A(T) from polynomial approximation given in Weast (1986; p. F5; eq. 1).

TRUE VALUES: True density values presented in Clark (1966; pp. 374-375).

CORRECTION: Difference between A(T) and true value.

GENERAL EQUATION: D = A(T) + 0.00233

TABLE 3. VISCOSITY OF PURE WATER AT DIFFERENT TEMPERATURES AND PRESSURES

TEMPERATURE VS. VISCOSITY OF PURE WATER AT DIFFERENT PRESSURES

		VISCOSITY (poise)			
		EMPIRICAL EQUATION	TRUE VALUES		
TEMP. (C)	C(T)	1 BAR	CORREC- TION	100 BAR	CORREC- TION
20	0.01002	0.01002	0.00000		
30	0.00798	0.00798	0.00000		
40	0.00653	0.00653	0.00000		
50	0.00547				
60	0.00467	0.00466	-0.00001		
70	0.00404				
80	0.00355	0.00354	-0.00001		
90	0.00315				
100	0.00282	0.00282	0.00000	0.00287	0.00006
110	0.00254				
120	0.00231	0.00232	0.00001		
130	0.00212				
140	0.00194				
150	0.00180				
PRESSURE (BAR):		1		100	
AV. CORRECTION:		0.00000		0.00006	

NOTES

EMPIRICAL EQUATION: C(T) from approximation given in Weast (1986, p. F-37)

TRUE VALUES: True viscosity values presented in Clark (1966; p. 300)

CORRECTION: Difference between C(T) and true value.

TABLE 4. EXAMPLE SIMULATION PERFORMED IN THIS STUDY

Number of elements: 26

Number of nodes: 27

Elevation at upper boundary: -280 m MSL (Priest Rapids IF)

Elevation at lower boundary: -800 m MSL (Grande Ronde 5 IF)

Temperature at upper boundary: 31 degrees C

Temperature at lower boundary: 48 degrees C

Temperature distribution: linear (geothermal gradient)

Salinity at upper boundary: 400 mg/l

Salinity at lower boundary: 1200 mg/l

Salinity distribution: linear

Prescribed fresh water head at upper boundary: 122 m MSL (approximately equal to water levels in Wanapum and Grande Ronde piezometers)

Prescribed fresh water head at lower boundary: adjusted until piezometer water level at bottom of flow system approximately 1.0 meters higher than at top of system [$hw(N) - hw(0) = 1.0$].

Reference density: 1 g cm^{-3}

Intrinsic permeability: $1.0 \times 10^{-14} \text{ cm}^2$

Acceleration of gravity: 980 cm s^{-2}

Weighting factor: 0.8

TABLE 5. PRINTOUT FROM EXAMPLE SIMULATION

GEOTHERMAL GRADIENT: $\Delta T(\text{m})/\Delta H(\text{m}) = 1.0$; LINEAR SALINITY

TOP TEMP (C)	31	REF. DENS. (g/cm3)	1	VERT INTRINSIC PERM (cm2)	1.0E-14
BOT. TEMP (C)	48	NUMBER ELEMENTS	26	GRAVITY (cm/s2)	980
TOP EL (m MSL)	-120	PREDICTOR FACTOR	0.8		
BOT. EL (m MSL)	-800				
TOP SAL. (mg/l)	400	TOP REF. HEAD	122		
BOT. SAL. (mg/l)	1200	BOT. REF. HEAD	121.148		

ELEMENT	MID POINT		PURE WATER		NET		R	CURR. H	DH/DZ	M	PRED. H	PRED. H
	ELEV	TEMP.	VISCOS.	DENSITY	SALINITY	DENSITY						
	(m MSL)	(deg C)	(poise)	(g/cm3)	(mg/l)	(g/cm3)	()	(m MSL)	()	(gm/s/cm2)	(m MSL)	(m MSL)
								122.000				122
1	-290	31.32492	0.007755	0.99757	415.38461	0.99798	-0.00201	122.027	-1.373E-03	4.26186E-12	4.26186E-12	122.027
2	-310	31.95076	0.007659	0.99736	446.15384	0.99781	-0.00219	122.051	-1.153E-03	4.26186E-12	4.26186E-12	122.051
3	-330	32.63461	0.007547	0.99715	476.92307	0.99763	-0.00237	122.069	-9.297E-04	4.26186E-12	4.26186E-12	122.069
4	-350	33.26846	0.007447	0.99694	507.69230	0.99745	-0.00255	122.083	-7.049E-04	4.26186E-12	4.26186E-12	122.083
5	-370	33.94230	0.007348	0.99672	538.46153	0.99726	-0.00274	122.093	-4.757E-04	4.26186E-12	4.26186E-12	122.093
6	-390	34.59615	0.007252	0.99650	569.23076	0.99707	-0.00293	122.098	-2.449E-04	4.26186E-12	4.26186E-12	122.098
7	-410	35.25	0.007158	0.99628	600	0.99688	-0.00312	122.098	-1.142E-05	4.26186E-12	4.26186E-12	122.098
8	-430	35.90584	0.007066	0.99605	630.76923	0.99668	-0.00332	122.093	2.246E-04	4.26186E-12	4.26186E-12	122.093
9	-450	36.55769	0.006975	0.99582	661.53846	0.99648	-0.00352	122.084	4.631E-04	4.26186E-12	4.26186E-12	122.084
10	-470	37.21153	0.006887	0.99558	692.30769	0.99627	-0.00372	122.070	7.043E-04	4.26186E-12	4.26186E-12	122.070
11	-490	37.86538	0.006800	0.99534	723.07692	0.99607	-0.00393	122.051	9.479E-04	4.26186E-12	4.26186E-12	122.051
12	-510	38.51923	0.006715	0.99510	753.84615	0.99586	-0.00414	122.027	1.194E-03	4.26186E-12	4.26186E-12	122.027
13	-530	39.17307	0.006632	0.99486	784.61538	0.99564	-0.00435	121.998	1.443E-03	4.26186E-12	4.26186E-12	121.998
14	-550	39.82692	0.006551	0.99461	815.38461	0.99543	-0.00457	121.964	1.694E-03	4.26186E-12	4.26186E-12	121.964
15	-570	40.48076	0.006471	0.99436	846.15384	0.99521	-0.00479	121.925	1.948E-03	4.26186E-12	4.26186E-12	121.925
16	-590	41.13461	0.006392	0.99411	876.92307	0.99498	-0.00501	121.881	2.204E-03	4.26186E-12	4.26186E-12	121.881
17	-610	41.78846	0.006316	0.99385	907.69230	0.99476	-0.00524	121.832	2.463E-03	4.26186E-12	4.26186E-12	121.832
18	-630	42.44230	0.006241	0.99359	938.46153	0.99453	-0.00547	121.778	2.724E-03	4.26186E-12	4.26186E-12	121.778
19	-650	43.09615	0.006167	0.99333	969.23076	0.99429	-0.00570	121.718	2.987E-03	4.26186E-12	4.26186E-12	121.718
20	-670	43.75	0.006094	0.99306	1000	0.99406	-0.00594	121.653	3.253E-03	4.26186E-12	4.26186E-12	121.653
21	-690	44.40384	0.006023	0.99279	1030.7692	0.99382	-0.00617	121.582	3.522E-03	4.26186E-12	4.26186E-12	121.582
22	-710	45.05769	0.005954	0.99252	1061.5384	0.99358	-0.00642	121.507	3.793E-03	4.26186E-12	4.26186E-12	121.507
23	-730	45.71153	0.005886	0.99224	1092.3076	0.99333	-0.00666	121.425	4.066E-03	4.26186E-12	4.26186E-12	121.425
24	-750	46.36538	0.005819	0.99196	1123.0769	0.99309	-0.00691	121.338	4.342E-03	4.26186E-12	4.26186E-12	121.338
25	-770	47.01923	0.005753	0.99168	1153.8461	0.99284	-0.00716	121.246	4.620E-03	4.26186E-12	4.26186E-12	121.246
26	-790	47.67307	0.005688	0.99140	1184.6153	0.99258	-0.00741	121.148	4.900E-03	4.26186E-12	4.26186E-12	121.148
AVERAGE												
4.26186E-12												

TABLE 5. (cont.)

NODE	NODE ELEV (m MSL)	TEMP. (C)	PURE WATER DENSITY (g/cm)	SALINITY (mg/l)	NET DENSITY (g/cm)	PRESSURE (dyne/cm ²)	FRESH WTR HEAD (m MSL)	ENVIR HEAD (m MSL)	TRUE HEAD (m MSL)	PIEZO LEVEL (m MSL)
0	-280	31	0.99767	400	0.99807	3.9356E+07	122.000	122.777	122.777	122.806
1	-300	31.653846	0.99747	430.7652	0.99790	4.1359E+07	122.027	122.917	122.845	122.873
2	-320	32.307692	0.99726	461.5384	0.99772	4.3321E+07	122.051	123.061	122.912	122.927
3	-340	32.961538	0.99705	492.3076	0.99754	4.5283E+07	122.069	123.210	122.978	122.979
4	-360	33.615384	0.99683	523.0769	0.99735	4.7244E+07	122.083	123.363	123.044	123.030
5	-380	34.269230	0.99661	553.8461	0.99716	4.9205E+07	122.093	123.521	123.168	123.079
6	-400	34.923076	0.99639	584.6153	0.99697	5.1166E+07	122.098	123.683	123.172	123.127
7	-420	35.576923	0.99616	615.3846	0.99678	5.3126E+07	122.098	123.851	123.235	123.174
8	-440	36.230769	0.99593	646.1538	0.99658	5.5085E+07	122.093	124.023	123.297	123.219
9	-460	36.884615	0.99570	676.9230	0.99638	5.7044E+07	122.084	124.201	123.358	123.262
10	-480	37.538461	0.99546	707.6923	0.99617	5.9003E+07	122.070	124.384	123.419	123.304
11	-500	38.192307	0.99522	738.4615	0.99596	6.0961E+07	122.051	124.573	123.479	123.345
12	-520	38.846153	0.99498	769.2307	0.99575	6.2919E+07	122.027	124.767	123.538	123.385
13	-540	39.5	0.99473	800	0.99553	6.4876E+07	121.998	124.967	123.597	123.423
14	-560	40.153846	0.99449	830.7692	0.99532	6.6833E+07	121.964	125.173	123.655	123.460
15	-580	40.807692	0.99423	861.5384	0.99509	6.8789E+07	121.925	125.385	123.712	123.496
16	-600	41.461538	0.99398	892.3076	0.99487	7.0744E+07	121.881	125.604	123.768	123.530
17	-620	42.115384	0.99372	923.0769	0.99464	7.2700E+07	121.832	125.829	123.824	123.563
18	-640	42.769230	0.99346	953.8461	0.99441	7.4654E+07	121.778	126.059	123.879	123.595
19	-660	43.423076	0.99319	984.6153	0.99418	7.6608E+07	121.718	126.296	123.934	123.626
20	-680	44.076923	0.99292	1015.384	0.99394	7.8562E+07	121.653	126.540	123.988	123.655
21	-700	44.730769	0.99265	1046.153	0.99370	8.0515E+07	121.582	126.791	124.042	123.683
22	-720	45.384615	0.99238	1076.923	0.99346	8.2468E+07	121.507	127.049	124.095	123.710
23	-740	46.038461	0.99210	1107.692	0.99321	8.4420E+07	121.425	127.314	124.147	123.736
24	-760	46.692307	0.99182	1138.461	0.99296	8.6371E+07	121.338	127.586	124.199	123.760
25	-780	47.346153	0.99154	1169.230	0.99271	8.8322E+07	121.246	127.865	124.250	123.784
26	-800	48	0.99125	1200	0.99245	9.0273E+07	121.148	128.151	124.301	123.806

FIGURE 1. TEMPERATURE VS DENSITY OF PURE WATER AT DIFFERENT PRESSURES

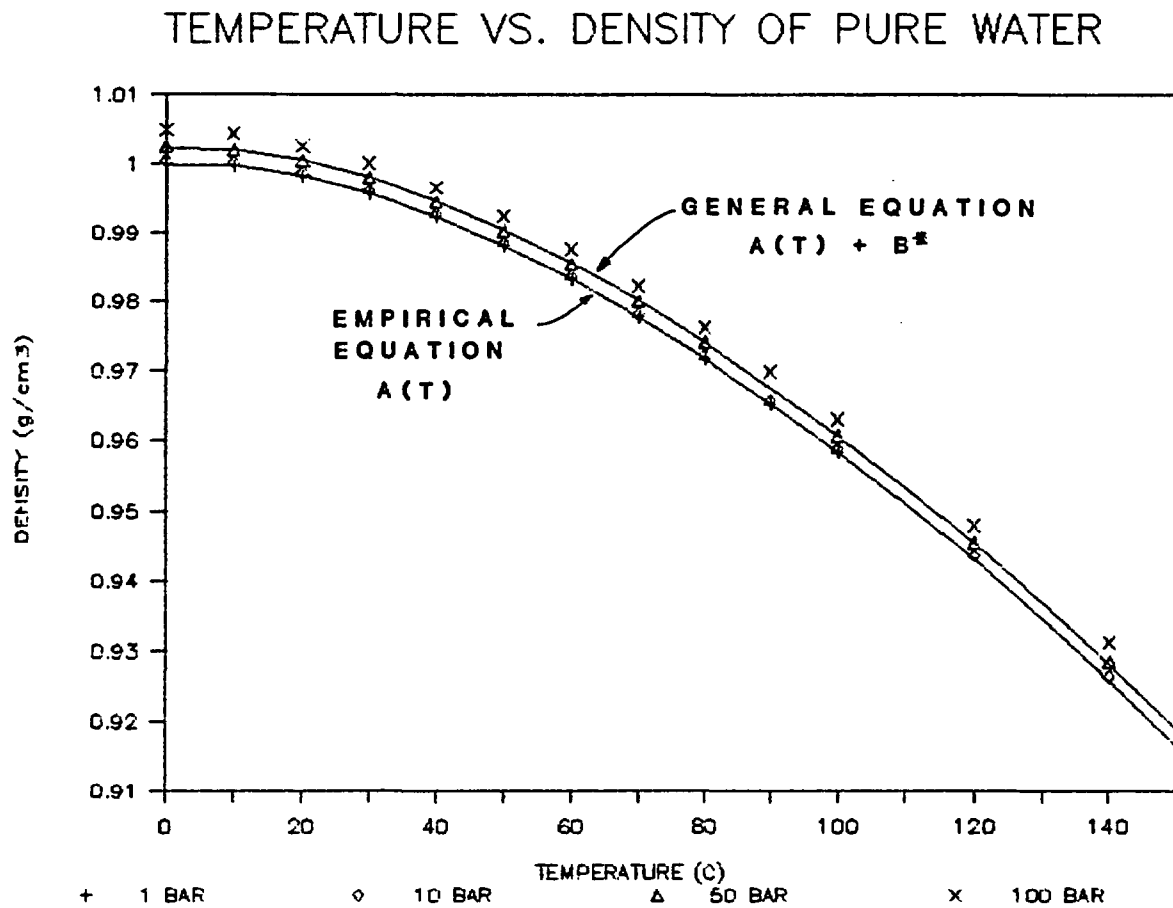


FIGURE 2. PRESSURE CORRECTION FOR DENSITY OF PURE WATER

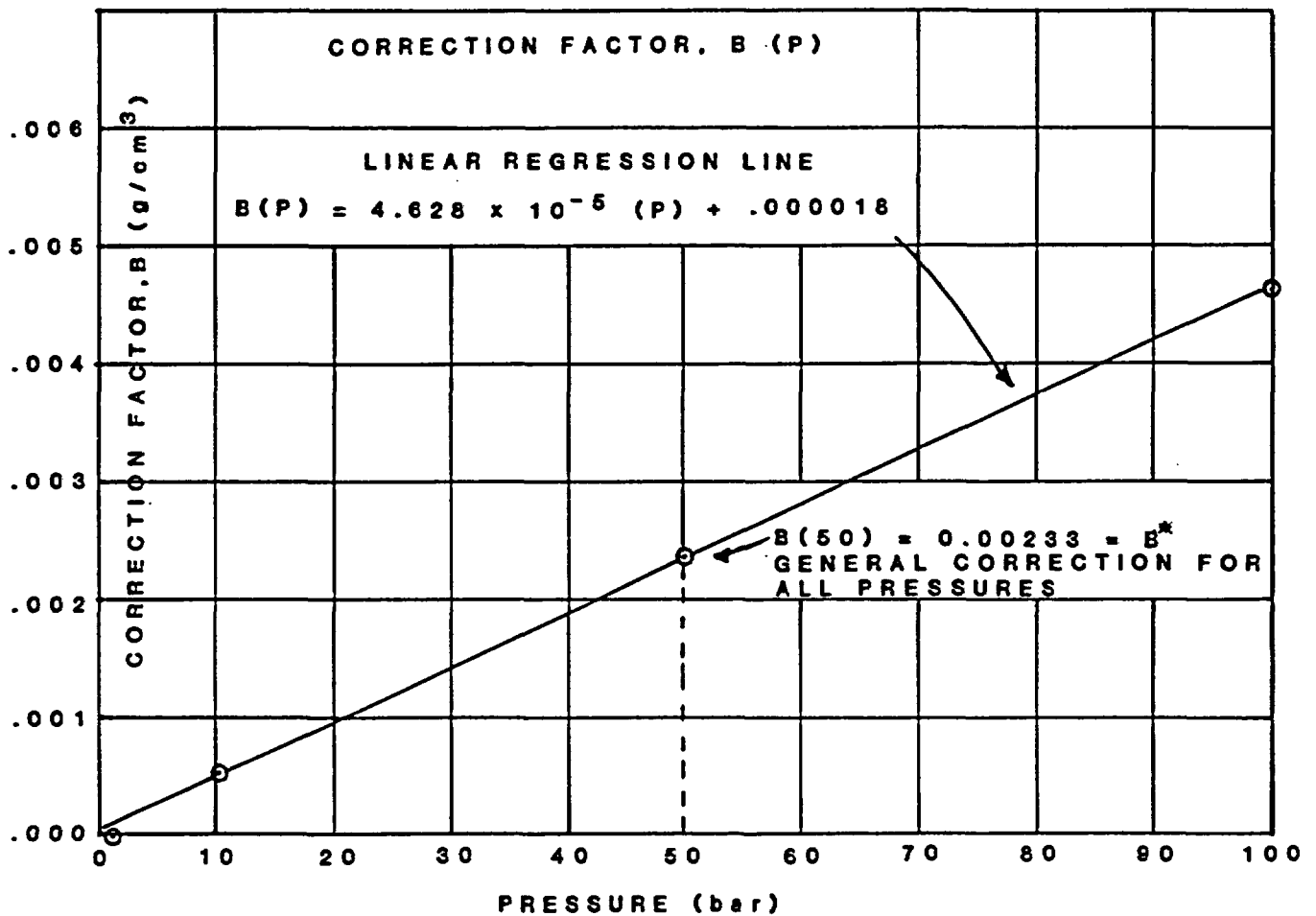


FIGURE 3. TEMPERATURE VS. VISCOSITY OF PURE WATER

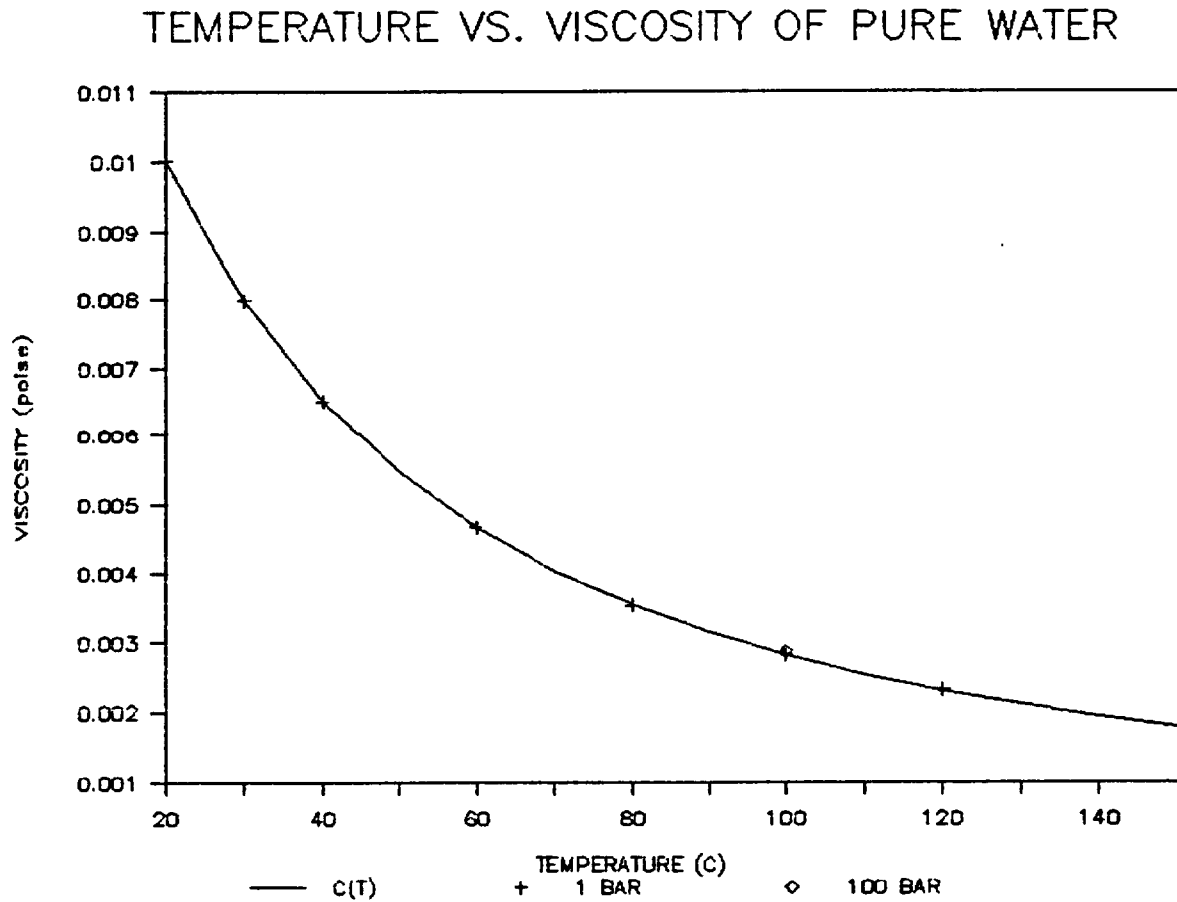


FIGURE 4. FINITE DIFFERENCE DISCRETIZATION

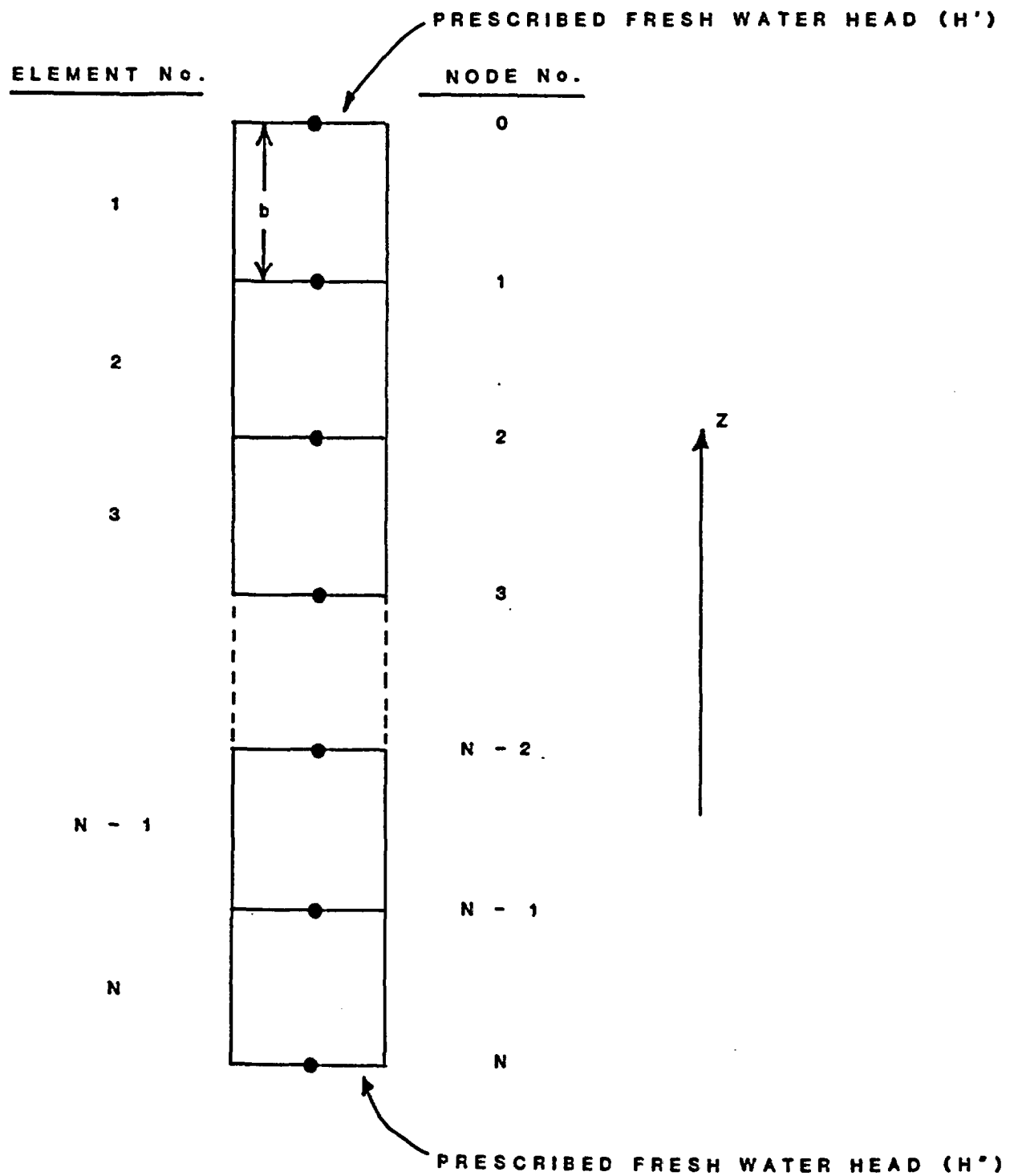


FIGURE 5. ITERATIVE SOLUTION FLOW CHART

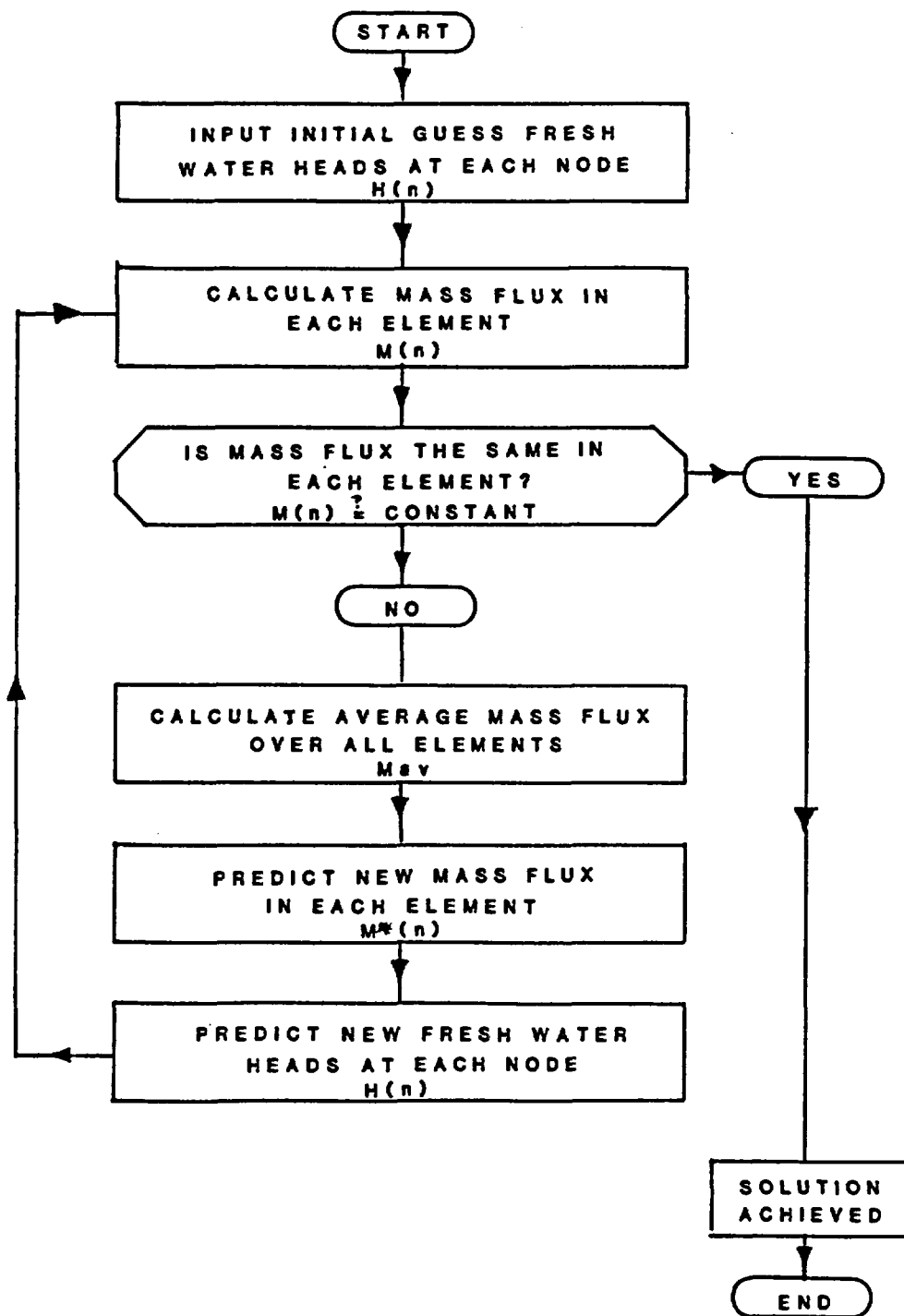


FIGURE 6. FINITE DIFFERENCE MODEL USED IN EXAMPLE SIMULATION

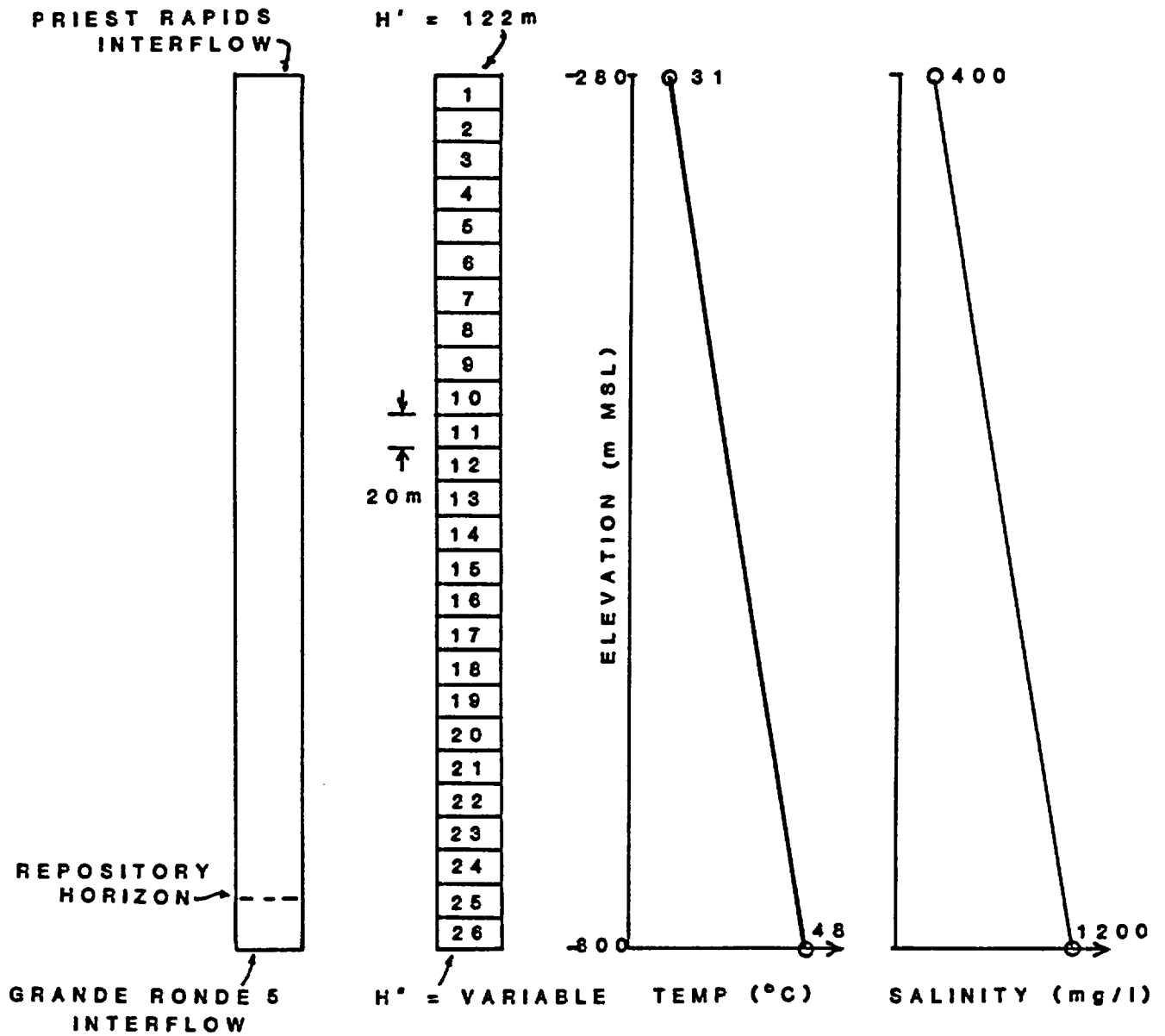


FIGURE 7. HEAD PLOTS FROM EXAMPLE SIMULATION

